Evolution of Particle-Void Fabric in Cyclic Liquefaction of Granular Soils: Insights from Discrete Element Modeling

Gang Wang[a], Jiangtao Wei[a] and Duruo Huang[b]

[a] *Department of Civil and Environmental Engineering, Hong Kong University of Science and Technology, Clear Water Bay, Kowloon, Hong Kong*
[b]*Department of Civil and Environmental Engineering and Institute for Advanced Study, Hong Kong University of Science and Technology, Clear Water Bay, Kowloon, Hong Kong*
* gwang@ust.hk (*corresponding author's E-mail)*

Abstract

Discrete element modeling (DEM) provides significant insight into the fundamental mechanism of soil liquefaction. In this study, a series of undrained cyclic simple shear simulations were conducted to study particle-void distribution of granular assemblages during pre- and post-liquefaction processes using DEM. The particle-scale information provided by DEM was used to quantify the local void distribution around particles. Two micro-scale descriptors, E_d and A_d, were proposed to quantify the overall anisotropy of the particle-void fabric in terms of the shape and orientation of local void distribution, respectively. Before initial liquefaction, the particle-void fabric remains to be globally isotropic. An irreversible development of the fabric anisotropy mainly occurs in the post-liquefaction stage. It was observed that jamming transition of the liquefied soil, i.e., transformation from a fluid-like flow state to a solid-like hardening state, can be uniquely determined by these descriptors. Furthermore, large flow deformations were found to be closely correlated to the particle-void fabric. The discrete element modeling provides insightful observation that links microscopic fabric evolution to macroscopic behavior of soils in the liquefaction process, which is useful for the development of constitutive models.

Keywords: Soil liquefaction; Particle-void fabric; Jamming transition; Discrete-element modeling

1. Introduction

For saturated granular soils under undrained cyclic loading, cyclic mobility and flow liquefaction may induce large ground deformation and cause severe damage to civil structures. Initial liquefaction refers to the first time when effective confining stress decreases to zero and excess pore water pressure ratio increases to 100% [1]. The overall undrained cyclic loading process can be separated into pre- and post-liquefaction stage by the initial liquefaction. In the post-liquefaction stage, granular soils experience large flow deformation in a "fluid-like" state under nearly zero effective stress [2]. Jamming transition could occur in the liquefied soil, leading to a hardening state or "solid-like" state under non-zero effective stress [3]. Traditional studies on fabric quantification are mostly based on inter-particle contacts. However, the construction of the void cell is still based on either branch vectors [4] or inter-particle contacts, which is only useful to quantify the anisotropy of void in a "solid-like" state, but not the "fluid-like" state after initial liquefaction [5-7].

In this paper, two new void-based fabric measures, E_d and A_d, are developed to characterize the shape and orientation of local void distribution around particles. Evolution of the two new fabric measures are investigated for granular soils over the whole liquefaction process through a series of undrained cyclic simple shear tests using the DEM. Post-liquefaction behaviors, in terms of jamming transition and flow deformation, are correlated to these new descriptors. The micromechanical modeling aims at providing insight into the fundamental mechanism of soil liquefaction.

2. DEM Simulation of Cyclic Behavior of Granular Soils

In this study, Yade is used to conduct DEM simulation for investigating cyclic behavior of granular soils [8]. A total of 4000 circular 2D particles are generated randomly within a squared representative volume element (RVE). The radius of particles ranges from 0.15 mm to 0.45mm, while

the mean radius R_{50} is 0.3 mm, associated with a Young's modulus of 70 GPa and Poisson's ratio of 0.3. Periodic boundary condition is prescribed on this RVE to ensure the shear strain field uniform inside the RVE even when a relative small number of particles are used. The simplified Hertz-Mindlin model is used to describe the inter-particle contact behaviors in loading and unloading [9].

The particles are initially consolidated under a confining pressure of 100 kPa, then are subjected to undrained cyclic simple shear tests. The model set up is shown in Fig. 1(a). The cyclic shear stress ratio (CSR) is defined as the cyclic shear stress (τ) divided by the vertical consolidation stress ($\sigma'_{v,0}$ =100 kPa) [2]. Fig. 1(b) and (c) show the simulation results of a sample with its relative density of 62%. It should be noted that "relative density" used in this study is only a nominal terminology to indicate different denseness of the packing, and it does not have the same meaning as that used in the laboratory. It can be observed that with increasing cycle numbers, the effective vertical stress (σ'_v) gradually decreases until initial liquefaction occurs. The initial liquefaction is based on the occurrence of zero effective vertical stress, practically, σ'_v <0.5 kPa. After liquefaction, stress path shows repeated "butterfly" loops while the shear strain amplitude keeps increasing cycle by cycle. Fig. 1(d) shows the granular packing transforming between a flow state and a hardening state within a loading cycle in post-liquefaction stage. The shear deformation is divided into flow strain and hardening strain [3], as shown in Fig. 1(d). The flow strain (γ_0) refers to the double-amplitude strain component when shear stiffness is extremely low and effective stress is almost zero. During flow state, granular packing behaves like "fluid". The hardening strain (γ_0) refers to the strain component when shear stiffness and effective stress have a sharp increase or be much higher than zero. During hardening state, granular packing behaves like "solid". Note that before initial liquefaction, granular packing belongs to hardening state. The jamming transition point (point b in Fig. 1(d)) represents the end of the flow strain and the start of the hardening strain. At the hardening state, stress strain behavior is almost identical between different loading cycles, while flow strain amplitude increases cycle by cycle.

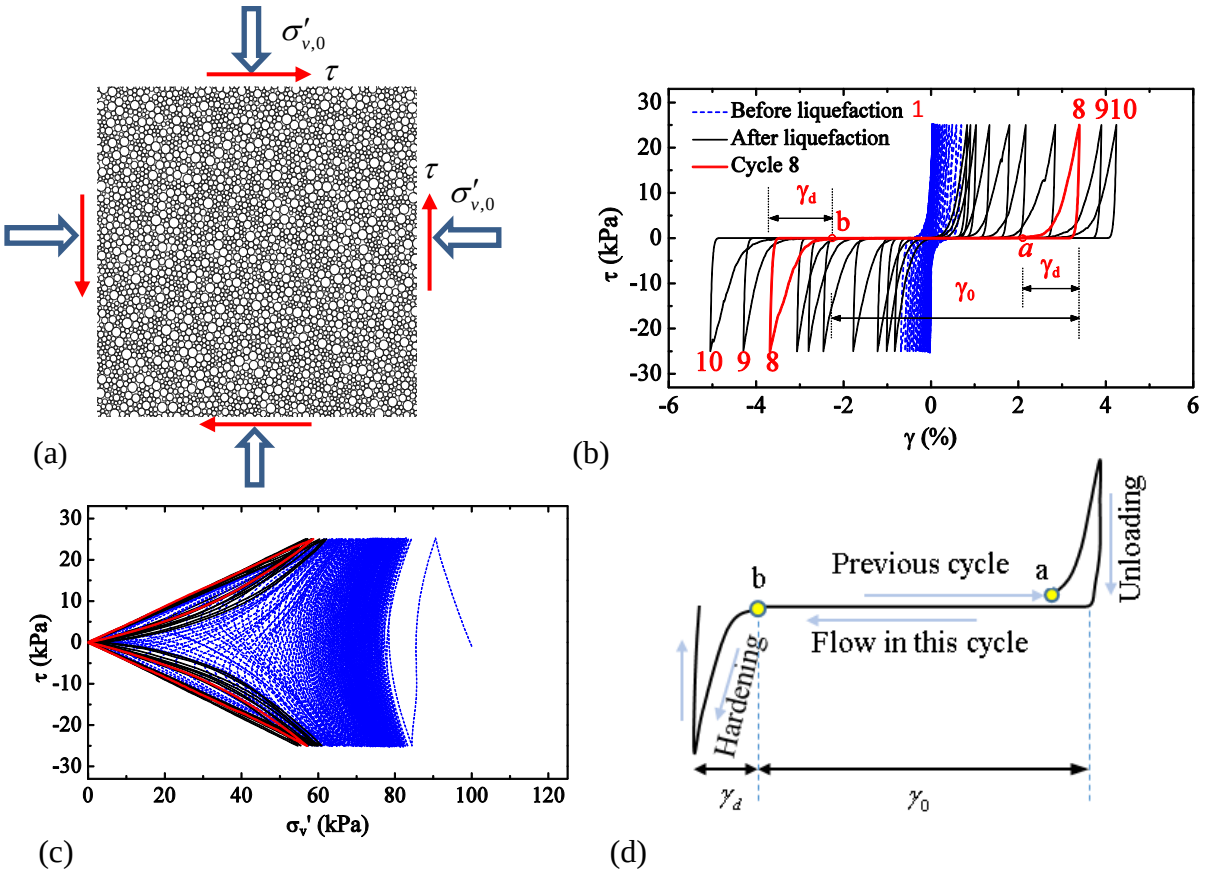

Fig. 1. Cyclic stress-strain behaviors of a sample with its relative density of 62%, and CSR of 0.25: (a) Model setup, (b) Shear stress and strain curve, (c) stress path, (d) definition of the flow strain and hardening strain. The cycle number is counted from initial liquefaction.

3. Particle-Void Fabric Descriptors

In this study, the weighted Voronoi tessellation is used to partition the void space around a particle (Fig. 2 (a)). The cell to particle ratio, $r(\theta)$, describes the angular distribution of the ratio between the radial dimension of the cell and the particle. Fourier approximation is used to quantify local anisotropy of $r(\theta)$ as follows:

$$r^2(\theta) = \frac{A}{\pi}\left[1 + e_d \cos 2(\theta - \theta_d)\right] \tag{1}$$

where A is the enclosed area of $r(\theta)$, e_d is the shape factor controlling the elongation of the void space. θ_d is the principal orientation of the shape. It is also worth pointing out the importance of shape factor (e_d) to mechanical behaviors of granular packing. For example, two granular packings with the same void ratio but different e_d values can result in different load-bearing structures: Particles forming an arching structure, capable of taking loads and behaves like a "solid" has a large e_d; on the other hand, particles are separated from each other, cannot take any load and behave like a "fluid" has a very small e_d value.

In this study, a new fabric descriptor measure is developed by statistically analyzing (e_d, θ_d) for all particles to quantify the partial-void distribution in a granular packing. The first descriptor E_d is defined as the mean value of e_d,

$$E_d = \frac{1}{N_p}\sum_{i=1}^{N_p} e_d^{(i)} \tag{2}$$

where N_p is the number of particles in the packing. Ideally, the probability density function (PDF) of e_d should be used to fully describe the distribution of the shape factor $\{e_d\}$. Yet, it is interesting to observe that the PDF of the normalized shape factor (e_d / E_d) follows a gamma distribution, which remains to be unchanged for samples under various loading stages.

On the other hand, the angular distribution function of θ_d for all particles, $f(\theta_d)$, can be expressed as:

$$f(\theta_d) = \frac{1}{2\pi}\left[1 + |A_d| \cos 2(\theta_d - \Theta_d)\right] \tag{3}$$

where $|A_d|$ quantifies the anisotropy degree of $f(\theta_d)$; $\Theta_d \in (0, \pi)$ is the principal direction of $f(\theta_d)$. The sign of A_d is determined by Θ_d such that when $\Theta_d \in (0, \pi/2)$, $A_d > 0$ and when $\Theta_d \in (\pi/2, \pi)$, $A_d < 0$.

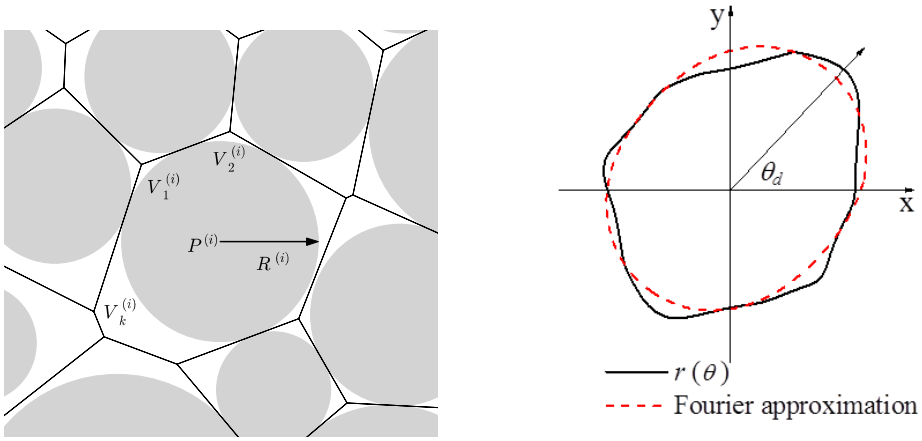

Fig. 2. Voronoi tessellation of particle-void cell and Fourier approximation of the void space

4. Particle-Void Evolution and Jamming Transition in Pre- and Post-Liquefaction

4.1 Evolution of E_d and A_d

Descriptors E_d and A_d are derived from statistical analysis of shape factor and principal direction associated with all particles in the packing to quantify the particle-void fabric. The evolution of the descriptors before and after initial liquefaction is examined. Fig. 3 shows the evolution of E_d and A_d versus the number of loading cycles under different CSRs. It can be observed that before initial liquefaction, the change in the fabric descriptors is negligible, while it becomes significant after the initial liquefaction. During the eight loading cycles after initial liquefaction, E_d decreases from 0.133 to 0.105 while the amplitude of A_d increase from 0.03 to 0.6. Afterwards, evolution of both E_d and A_d get stabilized. Within each loading cycle, E_d changes from 0.105 to 0.117 and A_d varies from -0.6 to 0.6, indicating the existence of an ultimate state of particle-void distribution. The decrease in E_d means that local void distribution around single particle (e_d) on average becomes less anisotropic.

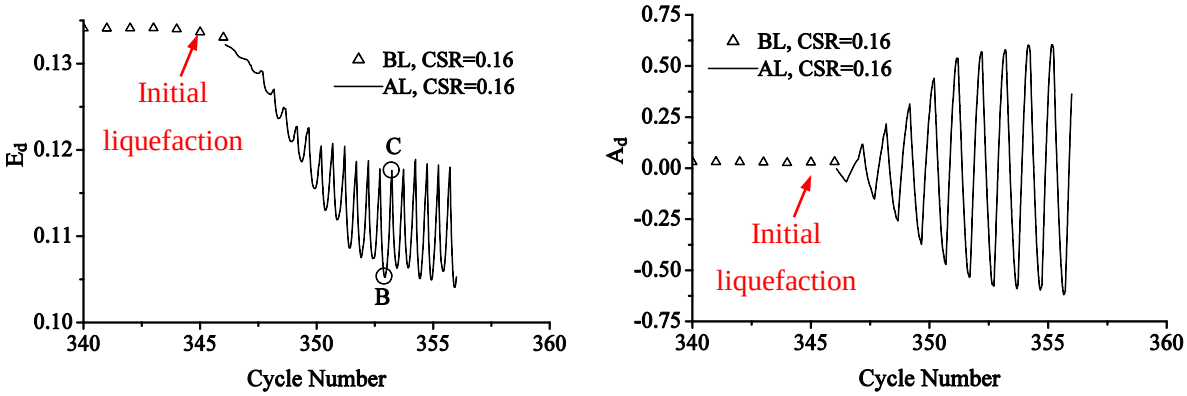

Fig. 3. The evolution of E_d and A_d versus numbers of cyclic loading during post-liquefaction

4.2 Jamming transition

In the post-liquefaction stage, granular packing will transform from a fluid-like flow state to a solid-like hardening state under shearing, a phenomenon called "jamming transition" actively studied in the physics community. The transition point is defined to separate the flow strain (γ_0) and the hardening strain (γ_d) as shown in Fig. 1(d). To identify the transition points, coordination number Z, defined as the ratio between total inter-particle contact number and total particle number, can be used to differentiate the mechanical status of granular packing [5,7, 10].

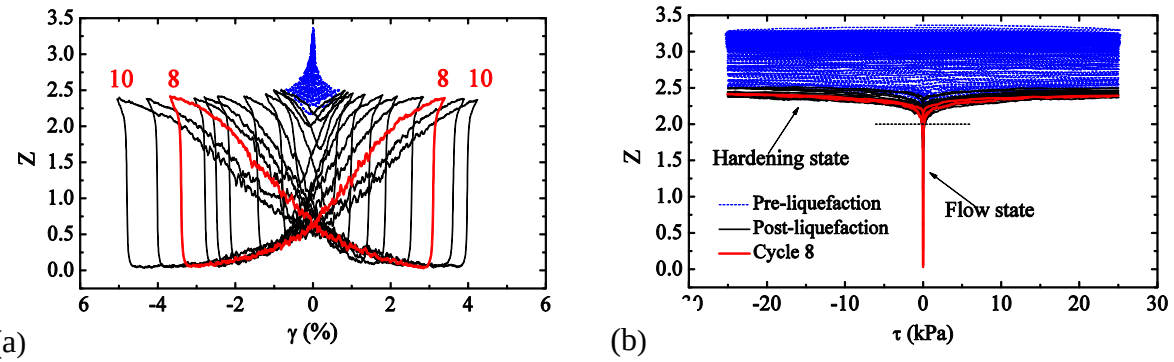

(a) (b)

Fig. 4. Coordination number Z of sample Dr=62% with CSR=0.25. (a) Z vs. strain curve, and (b) relation between Z and shear stress.

Fig. 4 shows evolution of Z during cyclic loading and the relation between Z and shear stress. It can be observed that before liquefaction, Z gradually decreases from initial value of 3.4 to 2.2 at the initial liquefaction. With further cyclic loading in post-liquefaction, Z shows a strong variation within each loading cycle. Strong correlation can be observed between Z and the shear stress in that the shear stress is negligible until Z is greater than a critical value of around 2. On average, a 2D particle needs at least two contacts with neighboring particles to establish a stable load-bearing structure in this sample. Similar observation was made from other two samples with different relative densities (Dr=46% and Dr=74%). Therefore, Z=2 is adopted in the current study to identify the jamming transition points.

Fig. 5(a) shows evolution of two fabric measures E_d and A_d during cyclic loading for sample Dr=62%. Given that the change in E_d and A_d is negligible before initial liquefaction, we only plot data in the post-liquefaction stage. It can be observed that E_d decreases gradually with increasing of absolute A_d. The jamming transition point (Z = 2) and an intermediate point (Z = 1) are highlighted using red circles. Clearly, the jamming transition point defines loci of a hardening state line (HSL) in the E_d-A_d space. More importantly, the HSL can be approximated using a linear line, which delineates the boundary to separate the flow state and hardening state in the E_d-A_d space. Inside HSL, granular packing belongs to the flow state with no load-bearing structure and behaves like a fluid. Beyond HSL, granular packing belongs to the hardening state with the stable load-bearing structure and behaves like a solid. The existence of HSL also implies that the loading bearing structure in the post-liquefaction stage can be formed only if either E_d or $|A_d|$ becomes sufficiently large. Otherwise, the packing remains to be in a flow state.

Additionally, the uniqueness of HSL is examined using the same sample under cases with different cyclic stress ratios (CSR=0.22, 0.25 and 0.28). As can be seen in Fig. 5(b), data from different loading cases are aligned on a single HSL, indicating that the particle-void distribution at the transition points is independent of different loading paths. Besides, HSL is found to be influenced by relative densities of samples, which shifts to the left for samples with higher density as shown in Fig 5(c). On the other hand, the influence of relative density to the slope of the HSL is unimportant based on the computational results.

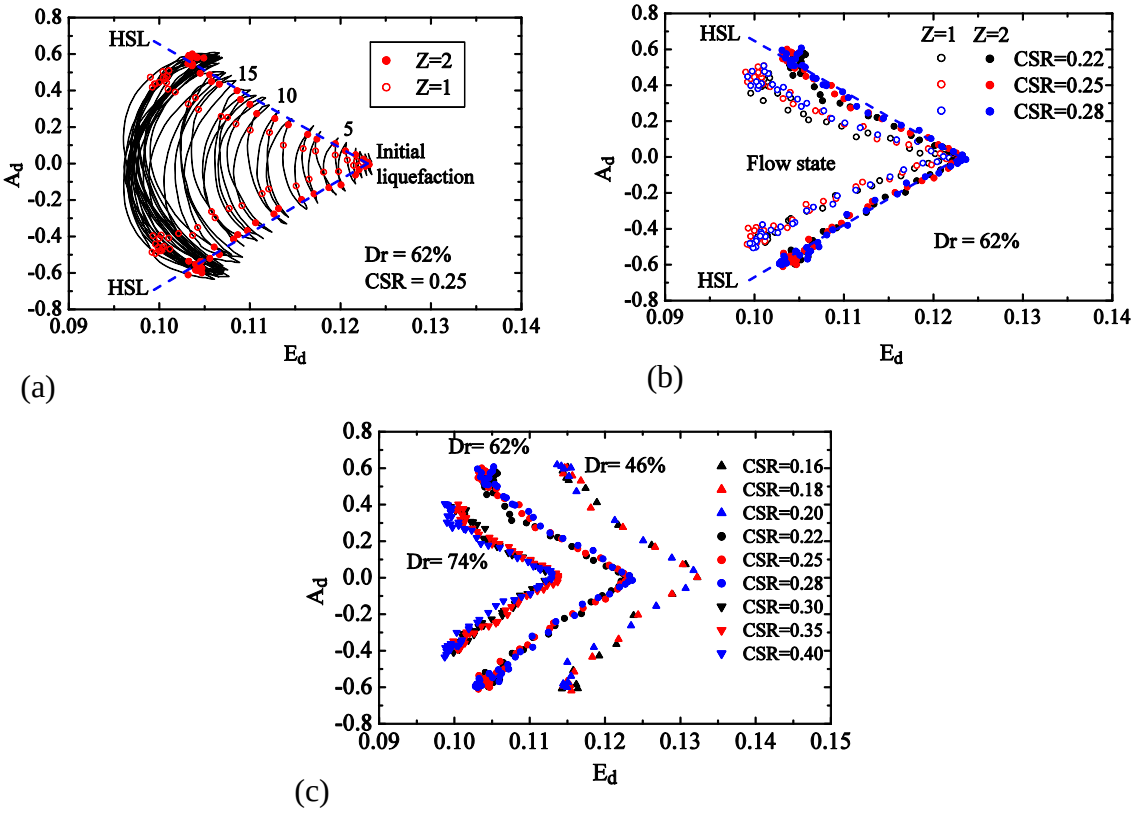

Fig. 5. (a) Evolution of E_d and A_d in the post-liquefaction stage, (b) Hardening state lines for different CSRs, (c) Hardening state lines for different samples with different CSRs

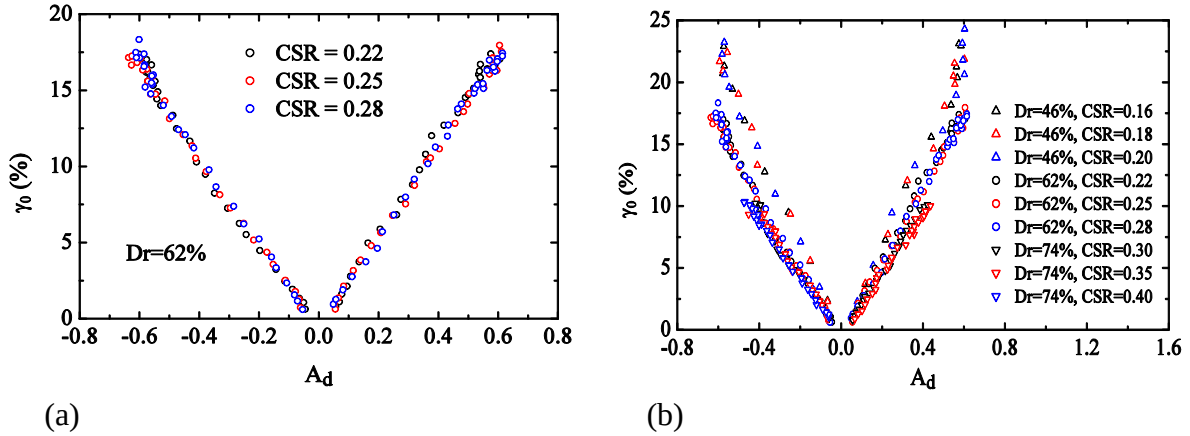

(a) (b)

Fig. 6. (a) The relationship between A_d at the unloading points and following flow strain amplitude γ_0 with different loading paths; (b) A_d - γ_0 relation of samples with different relative densities

4.3 Post-liquefaction flow strain

In the post-liquefaction stage, flow strain of median-to-dense sand accumulates quickly with more loading cycles performed, which is known as cyclic mobility. The flow stain amplitude in one cycle is the shear stain from unloading point to the next jamming transition point, as demonstrated in Fig. 1(d). In this study, the relationship between flow strain amplitude and the fabric descriptor A_d has been developed. Fig. 6(a) shows the A_d - γ_0 relation for a sample Dr=62% under different loading paths. A clear correlation can be observed between γ_0 and A_d, since data obtained from different loading paths align on two symmetric lines. It is also worth mentioning that the A_d - γ_0 relation is not influenced by different loading conditions. Fig. 6(b) shows the A_d - γ_0 relation for samples with different relative densities. It can be observed that the slope of A_d - γ_0 curves becomes steeper with decreasing relative density of samples.

5. Conclusions

In this study, two new fabric measures have been proposed to characterize the evolution of the particle-void fabric during cyclic liquefaction and cyclic mobility for 2D granular soils. A series of undrained cyclic simple shear tests have been conducted using discrete element method. It has been found that the particle-void distribution remains globally isotropic before initial liquefaction. An irreversible development of anisotropy in terms of E_d and A_d mainly occurs in the post-liquefaction stage, with gradually decreasing E_d and increasing A_d cycle by cycle.

Additionally, jamming transition of the liquefied soil is determined using these descriptors, as a unique hardening state line (HSL) is defined in the E_d-A_d pace which differentiates a post-liquefaction flow state from a hardening or jamming state. The existence of HSL demonstrates that the jamming transition in liquefied soils can occur only if either of the proposed two descriptors becomes adequately large. A strong correlation is also observed between $|A_d|$ and the post-liquefaction flow strain, indicating that the flow strain accumulates progressively with increasing $|A_d|$ cycle by cycle in the post-liquefaction stage. It is also worth pointing out the uniqueness of both HSL and the $|A_d|$ - γ_0 relation, which are found independent of different loading conditions for a packing. The discrete element modeling provides insightful observation that links microscopic fabric evolution to macroscopic behavior of soils in the liquefaction process, which is useful for the development of constitutive models.

Acknowledgements

This study was financially supported by Theme-based Research Scheme Grant No. T22-603-15N, General Research Fund No. 16213615 from the Hong Kong Research Grants Council and the discretionary fund from HKUST Jockey Club Institute for Advance Study.

References

[1] Seed HB, Lee KL. Liquefaction of saturated sands during cyclic loading. J Soil Mech Found Div ASCE 1996; 92(SM6): 105–134.
[2] Idriss I, Boulanger RW. Soil liquefaction during earthquakes, Monograph series, No. MNO-12. Oakland, CA, USA: Earthquake Engineering Research Institute 2008.
[3] Zhang JM, Wang G. Large post-liquefaction deformation of sand, part I: Physical mechanism, constitutive description and numerical algorithm. Acta Geotech 2012;7:69–113.
[4] Kuhn MR. Structured deformation in granular materials. Mech Mater 1999; 31(6): 407-429.
[5] Wang G, Wei J. Microstructure evolution of granular soils in cyclic mobility and post-liquefaction process. Granul Matter 2016:18(3): 51(1-13).
[6] Wei J, Wang G. Microstructure evolution of granular soils during liquefaction process. In: Geomechanics from Micro to Macro (eds K. Soga, K. Kumar, G. Biscontin and M. Kuo), pp. 251–256. London, UK: Taylor and Francis Group, 2015.
[7] Wei J, Wang G. Evolution of fabric anisotropy in cyclic liquefaction of sands. Journal of Micromechanics and Molecular Physics 2016; 1(3,4): 1640005.
[8] Šmilauer V. et al.. Using and Programming. In Yade Documentation 2nd ed. The Yade Project 2015, DOI 10.5281/zenodo.34043 (http://yade-dem.org/doc/)
[9] Yimsiri S, Soga K (2010). DEM analysis of soil fabric effects on behaviour of sand. Géotechnique 2010: 60(6): 483-495.
[10] Wei J, Wang G. Evolution of packing structure in cyclic mobility and post-liquefaction of granular soils. In: Bifurcation and degradation of geomaterials in the new millennium (eds K.T. Chau and J. Zhao), pp. 267-272. Springer Series in Geomechanics and Geoengineering. Hong Kong: Springer International Publishing 2015.